HHS Public Access

Author manuscript

*Clin Pharmacol Ther*. Author manuscript; available in PMC 2020 October 01.

Published in final edited form as:

*Clin Pharmacol Ther*. 2019 October ; 106(4): 821–830. doi:10.1002/cpt.1464.

# POPULATION MODELING HIGHLIGHTS DRUG DISPOSITION DIFFERENCES BETWEEN TENOFOVIR ALAFENAMIDE AND TENOFOVIR DISOPROXIL FUMARATE IN THE BLOOD AND SEMEN

**STEPHEN A. GREENE**[1], **JINGXIAN CHEN**[2], **HEATHER M.A. PRINCE**[3], **CRAIG SYKES**[4], **AMANDA P. SCHAUER**[4], **KIMBERLY BLAKE**[4], **JULIE A.E. NELSON**[5], **CYNTHIA L. GAY**[3], **MYRON S. COHEN**[3], **JULIE B. DUMOND**[4]

[1].AT TIME OF WORK: 4. CURRENT AFFILIATION: SK LIFE SCIENCE, INC, FAIR LAWN, NJ

[2].AT TIME OF WORK: 4. CURRENT AFFILIATION: MERCK CO, PHILADELPHIA, PA

[3].UNC SCHOOL OF MEDICINE, DEPARTMENT OF INTERNAL MEDICINE, DIVISION OF INFECTIOUS DISEASES, UNIVERSITY OF NORTH CAROLINA AT CHAPEL HILL, CHAPEL HILL, NC

[4].UNC ESHELMAN SCHOOL OF PHARMACY, DIVISION OF PHARMACOTHERAPY AND EXPERIMENTAL THERAPEUTICS, UNIVERSITY OF NORTH CAROLINA AT CHAPEL HILL, CHAPEL HILL, NC

[5].UNC SCHOOL OF MEDICINE, DEPARTMENT OF MICROBIOLOGY AND IMMUNOLOGY, UNIVERSITY OF NORTH CAROLINA AT CHAPEL HILL, CHAPEL HILL, NC

## Abstract

Understanding antiretroviral disposition in the male genital tract, a distinct viral compartment, can provide insight for HIV eradication. Population pharmacokinetic modeling was conducted to investigate the disposition of tenofovir disoproxil fumarate (TDF), tenofovir alafenamide (TAF), and emtricitabine and their metabolites in blood and semen. Blood plasma and seminal plasma (SP) concentrations of tenofovir and emtricitabine, and tenofovir-diphosphate and emtricitabine-triphosphate concentrations in the peripheral blood mononuclear cells (PBMC) and seminal mononuclear cells, were measured. Sequential compartmental modeling described drug disposition in blood and semen. Our modeling suggests slower apparent tenofovir-diphosphate

**CORRESPONDING AUTHOR:** JULIE B. DUMOND, PHARMD, MS, ASSISTANT PROFESSOR, DIVISION OF PHARMACOTHERAPY AND EXPERIMENAL THERAPEUTICS, UNC ESHELMAN SCHOOL OF PHARMACY, 1093 GENETIC MEDICINE BUILDING, 120 MASON FARM RD., CB 7361, CHAPEL HILL, NC 2759-7361 (919) 966-5017 JDUMOND@UNC.EDU.

AUTHOR CONTRIBUTIONS:

S.G., J.C., and J.D. wrote the manuscript; S.G., J.C., H.P., C.G., M.C., and J.D. designed the research; S.G., J.C., H.P., C.G., and J.D. performed the research; S.G., J.C., C.S., A.S., K.B., J.N., and J.D. analyzed the data.

DISCLOSURE

A version of this work has been previously presented at the 2017 American Conference on Pharmacometrics, October 15 – 18, Ft Lauderdale, FL, Abstract W-037.

CONFLICTS OF INTEREST

All other authors declared no competing interests for this work.

PBMC elimination and faster tenofovir SP elimination following TAF administration, compared to TDF, likely reflecting flip-flop kinetics. Additionally, TAF metabolism to TFV appeared slower in semen compared to blood; however, SP elimination of TAF-derived TFV appeared faster than its BP elimination. These findings provide valuable insight for further mechanistic study of cellular entry and drug metabolism in the male genital tract.

**Keywords**

HIV; Population Pharmacokinetics; Disposition; Antiretroviral

## INTRODUCTION

HIV-1 sanctuary sites are well-documented barriers to complete suppression of HIV replication (1,2,3). Considerable research effort is directed towards understanding viral and drug disposition within these sanctuary sites to inform research aimed at achieving HIV-1 cure. These immune-privileged sites include the central nervous system, lymph nodes, colorectal tissue, vaginal tissue, and the male genital tract (MGT), among others (1).

One strategy with some promise towards cure is known as the “kick and kill” approach. Here, latent virus is “kicked” out of latency into viral replication and thus made susceptible to antiretroviral (ARV) therapy. This strategy requires that the virus brought out of latency is presented with adequate concentration of drug for effective “killing”. Success of the “kick and kill” cure strategy hinges on the ability for both latency-reversing agents and antiretrovirals to adequately penetrate compartments such as the MGT (4). Thus, it is necessary to understand currently used ARV disposition within these sites. The MGT contains physiological barriers that protect sperm from potentially harmful xenobiotics. Sertoli cells serve as the primary cellular unit at this boundary; drug transporters such as P-glycoprotein (P-gp) expressed in these cells efflux xenobiotics back into the blood (3,5). Many drugs, including some ARVs (e.g. dolutegravir, darunavir, etravirine), exhibit low penetration into this compartment, relative to blood concentrations (6,7,8,9). In contrast, the nucleoside reverse transcriptase inhibitors (NRTIs) such as tenofovir (TFV) and emtricitabine (FTC) penetrate to a higher extent into this compartment in part due to the family of endogenous equilibrative nucleoside transporters (10); this class generally shows high seminal plasma (SP) concentrations relative to blood plasma (BP) (6).

Tenofovir (TFV) and emtricitabine (FTC) are commonly used NRTIs in HIV-1 treatment and pre-exposure prophylaxis (PrEP). TFV is available in two prodrug formulations, tenofovir disoproxil fumarate (TDF) and tenofovir alafenamide (TAF). They are distinct from one another, most notably in their metabolism to TFV and safety profiles. The driving force behind TDF-associated toxicity (renal impairment and bone density loss) is high TFV concentrations within the BP; post-absorption, TDF is cleaved to TFV, its main circulating form. TAF was developed to circumvent this by shifting the conversion of TAF to TFV into target cells, thus significantly decreasing BP concentrations of TFV and therefore, the risk of toxicity. Additionally, efficient cell loading of TAF drives higher concentrations of intracellular active drug, compared to TDF(11).

To more fully understand the pharmacokinetics (PK) within the blood and putative semen reservoir of HIV-positive and negative men taking TAF+FTC for treatment or TDF+FTC for treatment or PrEP, we developed a population PK model for TAF, TDF, and FTC with a focus on the differences between TAF and TDF with respect to blood and semen. A non-compartmental analysis (NCA) was conducted for all three drugs of interest and has been previously reported (12). In short, NCA revealed unexpected TFV PK differences between TAF and TDF in the semen. As expected, TFV BP median concentrations following TAF administration were markedly lower (~10-fold) than TFV median concentrations following TDF administration. However, TFV SP median concentrations were similar regardless of dosage form. Intracellular PBMC TFVdp median concentrations following TAF administration were approximately 6-fold higher, as expected, but in seminal mononuclear cells (SMCs) the median concentrations were similar irrespective of dosage form. To further describe these differences and inform future studies designed to probe the mechanisms, a population pharmacokinetic model for each of these prodrugs was built.

## RESULTS

### Population Pharmacokinetic Analysis: Model Structure and Performance

Figure 1 depicts the structural models of TDF and TAF; the structural model of FTC is included in the supplemental material. Goodness of fit (GoF) plots and model code for each of the models can also be found in the supplemental material.

**TDF—**A 5-compartment model (2 for BP, 1 for PBMCs, 1 for SP, and 1 for SMCs) with a fixed first order absorption rate constant and estimated first order elimination or disposition rate constants best described the TDF data. Two transit compartments between the BP and SP and a single transit between the BP and the SMCs improved model fitting and were retained in the final model. A transit compartment between the SP and SMCs was not supported by the data.

Final model and bootstrap estimates are presented in Table 1 with associated 95% confidence intervals (CIs) and relative standard error in percentage terms (%RSEs). Interindividual variability (ω, IIV) was placed on TFV CL/F and V/F in the BP as well as TFV elimination (K40) from the SP and TFVdp elimination (K50) from the SMCs. These were estimated with modest precision (<85 %CV) given the data limitation and the complexity of the model. Residual variability (a) was also estimated with modest precision (<55 %CV) apart from the SMC compartment, as this compartment had considerable variability within the data and many of the samples were pooled. Bootstrap estimates closely approximated the NONMEM estimates but the 95% confidence intervals (CI) and %RSE show low precision for these estimates for compartments outside of the blood plasma. Shrinkage on all inter-individual variability of CL/F, V/F, K40, and K50 were low (<30%).

Visual predictive checks (VPCs) for TDF are shown in Figure 2. VPCs demonstrate that the model generally captured the central tendency of the data, with high variability. Bootstrap estimates and %RSE values were determined from 561 successfully minimized models (56% success rate).

Additionally, initial TFVdp PBMC modeling revealed a single data point with a conditional weighted residual (CWRES) value > 6. This isolated data point was approximately 20-fold higher than the next concentration within the same subject. It was determined that this was likely due to a laboratory error, in that an incorrect cell count was recorded during sample processing. As a recount was not possible, this value was removed from analysis.

**FTC—**A 5-compartment model (2 for BP, 1 for PBMCs, 1 for SP, and 1 for SMCs) with a fixed first order absorption rate constant and estimated first order elimination or disposition rate constants best described the data obtained for FTC. A first order transit/conversion rate constant between the SP and SMCs was included in the model. No differences in PK for FTC when co-administered with the two TFV dosage forms, or differences between healthy and HIV-positive men were observed in the prior NCA. Thus, a single FTC model was developed.

Final model and bootstrap estimates with associated 95% CIs and %RSEs are presented in Supplemental Table 1 (Table S1). IIV estimates were placed on CL/F, V/F, K40, K25, K50, and K60 and all IIV estimates were low (<30 %CV) except for that associated with K60 (elimination from SMCs). Like TDF, residual variability (a) was also estimated with modest precision (<40 %CV) except for the error on the SMC compartment. The high variability estimates on both parameters result from highly variable data, with several pooled samples used to provide concentrations. Bootstrap estimates closely approximated NONMEM estimates with reasonable precision, as illustrated by the 95% CIs and %RSE values. %RSE values were high for IIV on K50, K60, and V/F. In general, less variability is present across all compartments compared to the TDF model and can be seen visually in the VPC plots. Shrinkage on all inter-individual variability parameters of CL/F, V/F, K40, K25, K50, and K60 were low (<30 %CV).

VPCs for FTC are shown in Supplemental Figure 2 (Figure S2). FTC VPCs show that the model captures the central tendency of the data with reasonable variability except for the SMC compartment. Bootstrap estimates and %RSE values were determined from 929 successfully minimized models (93% success rate).

**TAF—**Owing to differing TFV formation kinetics, a separate TAF model was constructed. A 5-compartment model (1 for TAF in BP, 1 for TFV in BP, 1 for PBMCs, 1 for TAF in SP, and 1 for TFV in SP) with an estimated first-order TAF absorption rate constant best described the data. Due to poor fitting and model instability, first-order transfer and conversion rate constants describing drug disposition between compartments were not supported. Instead, estimated relative transfer or conversion rates (relative to TAF elimination in the BP or SP) for drug disposition were used by multiplying the estimated elimination rate constant of TAF in the BP or SP by an estimated scalar constant. In addition, a lack of data in the SMC compartment precluded modeling TFVdp and was not included in the model, despite multiple attempts to incorporate it within the model framework. A two-compartment model was tested for TFV PK in the BP, but it did not improve overall model performance and thus a 1-compartment model was selected.

TAF model estimates can be found in Table 2. IIV was estimated for the relative rates K30, K40, K50, and K60. Most ω estimates (inter-individual variability) were high (range of 85 – 113 %CV) but were retained in the model due to model stability and improved GoF. Shrinkage on all inter-individual variability parameters of K30, K40, K50, and K60 were low (<30 %CV). Residual variability (a) was high (>45 %CV) for all compartments except for TFV in the BP, highlighting high variability present within the data.

TAF VPC plots (Figure 3) highlight a successful capturing of the central tendency of the data as well as the large variability in each modeled compartment. To increase the robustness of the model estimates and %RSE values derived from the bootstrap, all successfully minimized models and models that terminated due to rounding errors with > 1.5 significant digits were included (n=319; rate of 32%).

Median bootstrap estimates closely resembled NONMEM estimates with some estimates exhibiting high variability as illustrated by the large 95% CIs and high %RSE. Nonetheless, many of the estimates were relatively precisely estimated.

## Comparison of Final TDF and TAF Model Estimates

Table 3 shows a comparison of median TFV bootstrap parameters between TDF and TAF.

**Differences in TFV disposition between TDF and TAF—**Assuming a blood plasma volume of distribution of 2000 L, TFV CL from BP following TAF administration (K40*2000 L) is approximately 10% that of the TFV CL following TDF administration and is likely illustrative of the differing rate-limiting steps in the initial distribution of and conversion to TFV, rather than a different elimination pathway. Though the TFV transit rate from the BP to the PBMC between TDF (K24) and TAF (K23*K20) is similar, this comparison is difficult to interpret as the “transit” for TAF also includes intracellular conversion, demonstrated to be more efficient for TAF (13). TFVdp elimination rate constant from the PBMCs following TAF administration (K30) was estimated to be approximately 40% that of the TFVdp elimination rate constant from the PBMCs following TDF administration (K40). While both rates of elimination are slow, TFVdp elimination following TAF administration is slower; determining half-lives for these long-lived intracellular metabolites is difficult and estimates available in the literature vary widely (14). However, increased concentrations of TFVdp following TAF administration may result in saturation of TFVdp catabolism and contribute to this difference.

A comparison of the transit rate of TFV to the seminal plasma from the blood plasma following TDF (K25) and TAF (K46) administration reveals similar rates (0.0152 $hr^{-1}$ vs 0.00952 $hr^{-1}$) while TFV elimination rates from SP following TDF administration (K50) and TAF administration (K60) were quite different (0.0126 $hr^{-1}$ vs 1.97 $hr^{-1}$). This suggests that the apparent rate of TFV disappearance from the SP following TAF administration is significantly faster compared to TDF. This may potentially reflect its complex metabolism and transport rather than a different elimination mechanism.

### Differences in TAF conversion to TFV and TFV apparent elimination rate from blood and semen

A comparison of the TAF conversion to TFV in the BP and SP also revealed differences between the two biological matrices. The TAF conversion to TFV in the BP was estimated at 1.33 $hr^{-1}$ (K20*K24) while the conversion of TAF to TFV in the SP was estimated at 0.000327 $hr^{-1}$ (K50*K56). This slower conversion in the SP may be related to the fewer cells capable of converting the drug within the MGT (i.e., TAF to TFV to TFVdp). Additionally, the TFV elimination rate from the BP following TAF administration was estimated at 0.00230 $hr^{-1}$ (K40) compared to the elimination rate from the SP following TAF administration was estimated at 1.98 $hr^{-1}$ (K60). Faster SP elimination compared to BP elimination following TAF administration could be a result of destructive sampling plus differences in SP transport and metabolism. TAF is measurable in SP and cathepsin A is ubiquitous in the MGT tract, (15) potentially resulting in a cellular “sink”. TFV is also available systemically for transport into and out of the MGT; therefore, the complex routes of distribution for this compartment may contribute. In contrast, elimination of TFV from the BP and SP following TDF was estimated at 0.0545 ($CL_{tfv}$/[V/F + V2/F]) and 0092 (K50), respectively, implying that TFV distribution from the two fluids after TDF administration more closely resemble one another.

## DISCUSSION

In this study, we developed a population pharmacokinetic model for the antiretrovirals tenofovir TAF and FTC and their respective intracellular metabolites to relate drug and metabolite concentrations in the BP and PBMCs to those observed in the MGT. For each drug, intra- and extracellular compartments within the blood and semen were fit to measured concentrations. Several parameters were estimated with high variability, reflective of variation within the data and the small sample size. The high variability captured in the modeling highlights the heterogeneity present in the data across dosage forms. Model estimates derived from the TDF and TAF models were compared to each other. This exercise provided valuable insight into the dispositional differences between these two dosage forms with respect to extracellular TFV and intracellular TFVdp.

In comparing the estimates derived from this modeling for TDF and TAF, differences in drug disposition patterns between the two dosage forms were revealed. First, we estimated an apparent 10-fold difference in TFV CL/F from BP; estimates from recent single-dose studies in healthy volunteers (16) suggest that CL/F of TFV is similar regardless of dosage form. Other data, including data analyzed by Gilead Sciences,(17) support a longer half-life, slower clearance, and increased total volume of distribution of TFV following TAF administration. TAF is stable in BP and TFV is formed in target cells throughout the body then effluxed back into circulation, thus accounting for the increased volume of distribution compared to TDF-generated TFV, formed in the blood after absorption. (11,18,19). Our ability to accurately estimate TFV BP volume of distribution following TDF administration was limited, based on our sparse sampling scheme. Since the TFV concentrations in the BP following TAF administration arise from a separate pathway, the ability to accurately estimate TFV BP volume of distribution is likely an identifiability issue, as opposed to a

limitation of sample timing. Decreased TFV systemic clearance estimates observed with TAF administration are most likely due to flip-flop kinetics, where the formation and systemic distribution of TFV is the slower, rate limiting step and reflected in the concentration-time profile as the elimination rate. TFV has been measured in urine after TAF administration,(20) and thus it is unlikely that it is cleared by any process other than renal elimination, as observed with TDF-generated TFV. Given this, these clearance estimates should be interpreted with caution. Additional limitations specific to semen collection are the use of destructive sampling, low seminal cell yields, and, consequently, a high proportion of SMC TFVdp BLQ values.

The slower observed elimination of TFVdp from PBMCs following TAF administration compared to TDF administration has not been specifically quantified in the literature. Quantifying the half-life of these difficult to measure, long-lived moieties is challenging, and literature estimates vary. Our observation is likely to be attributed, at least in part, to the much higher TFVdp loading of the PBMCs following TAF administration and potential saturation of catabolic pathways.

Finally, our analysis revealed a much faster elimination of TFV from the SP following TAF elimination compared to TDF. This difference may be multifaceted (i.e., transporters, enzymatic breakdown, etc.) but the finding warrants further investigation. This finding is especially enlightening since our previously reported NCA showed similar TFV SP (and TFVdp SMC) concentrations across the two dosage forms (12).

Taken together, the NCA and population PK analyses suggest that despite similar concentrations of drug in SP and SMCs, the underlying mechanisms of the disposition of TFV and TFVdp in the MGT are different across dosage forms, as previously demonstrated for the blood (18). We hypothesize that the differences in rates observed for TFV do not suggest different elimination pathways, but rather, reflect its more complex formation and distribution following TAF administration. It is likely that the rate-limiting step of TFV formation following TAF administration is slower than its renal clearance, and thus, we are observing a phenomenon akin to flip-flop kinetics. These differences include an ~40% slower TFVdp elimination from the PBMCs following TAF administration compared to TDF administration, potentially reflecting saturation of catabolic enzymes; a faster disappearance of TFV from the SP following TAF compared to TDF (1.98 $hr^{-1}$ vs. 0.0126 $hr^{-1}$), likely reflecting complex metabolism and transport; and a smaller (~10%) TFV clearance from the BP following TAF administration compared to TDF administration (assuming a TFV volume of distribution in the BP of 2000L), likely reflecting the rate limiting steps in TFV formation and appearance in the systemic circulation rather than a true difference in clearance mechanisms. It should be noted that while these parameters are not directly interpretable from a physiologic stand point, they do highlight general mechanistic differences. Semi-physiologically- based PK analysis may lend itself well to these data for further exploration of mechanisms of TAF disposition in the male genital tract.(21)

## Conclusions

The observed differences in drug disposition between TAF and TDF in the MGT are likely multifaceted and our understanding of the underlying mechanisms is limited. The clinical

significance of these differences has yet to be elucidated; the small body of data on viral suppression in the MGT with TAF suggests adequate control from a treatment perspective, comparable to TDF (22). From a cure perspective, PK in viral compartments should be a consideration in drug development, with better mechanistic understanding of drug pharmacokinetics/pharmacodynamics and SMC physiology leveraged towards control of reactivated latent virus.

## METHODS

The clinical study conduct, as approved by the UNC Biomedical Institution Review Board, bioanalytical methods, and NCA were described in detail previously (12). Briefly, 16 HIV-positive and 8 HIV-negative men (total n=24) free from active sexually transmitted infections (aside from HIV) provided 6 samples over 48 hours and two doses to construct a composite 24-hour blood and semen drug concentration profile (post-dose hours 3, 6, 9, 12, 18, 24) for TFV, TFVdp, FTC and FTCtp.

Analytes were measured using LC/MS-MS methods in the UNC Center for AIDS Research Clinical Pharmacology and Analytical Chemistry Laboratory; for TFV and FTC in BP and SP, the dynamic range of the assay is 10–10,000 ng/mL, and for TFVdp and FTCtp in PBMCs and SMCs, the dynamic range of the assay is 0.02–2,000 ng/mL. These methods are fully validated, with calibrators and quality control samples within 15% of the nominal value for within-day and between-day runs. Parent TAF was measured in BP and SP by LC-MS/MS, using a research-only, partially validated analytical method. TAF concentrations were measured with a dynamic range of 0.100 – 100 ng/mL, with calibrators and quality control samples within 25% of the nominal value for within-day and between-day runs. For the intracellular concentrations, the sample volume and the cell count, along with the lower limit of quantification (LLOQ) of the assay (0.02 ng/mL), a sample-specific LLOQ was calculated for all intracellular concentrations.

Semen samples were centrifuged to separate SP from cellular content; SMCs were then separated from sperm cells using a density gradient. Once separated, SMCs were counted and frozen as a dry pellet. In order to increase sensitivity, SMC samples with <300,000 cells/mL were pooled within a participant. Thus, any intracellular concentrations measured from these subjects represented an average 24-hour concentration. All concentrations were subsequently converted to molar units with intracellular concentrations being calculated using an estimate for the volume of mononuclear cells of 282 fl/cell. (23)

### Population Pharmacokinetic Analysis

PopPK was performed using NONMEM version 7.3 (ICON Development Solutions, Hanover, MD). Data management, graphical analysis, and standard statistical analysis were conducted in R (version 3.1.0 or higher, r-project.org). Pirana (version 2.9.2) was used for model management and NONMEM output visualization. The ADVAN 6 routine and first order conditional estimation with interaction (FOCE-I) method (for TDF and FTC) or Laplacian with interaction method (for TAF) were used for parameter estimation.

**TDF and FTC—**For TDF and FTC, sequential modeling of the blood plasma, PBMCs, seminal plasma, and SMCs was performed. For TDF a total of 323 concentration values (n=96 for TFV in BP; n=92 for TFVdp in PBMCs; n=91 for TFV in SP; n=44 for TFVdp in the SMCs) were used in the TDF final model. For FTC a total of 464 concentration values (n=144 for FTC in BP; n=138 for FTCtp in PBMCs; n=133 for FTC in SP; n=49 for FTCtp in the SMCs) were used in the FTC final model. Intra- and extracellular disposition of TFV (from TDF) or FTC and their respective metabolites were linked between matrices with first order rate constants. Transit compartments were implemented when deemed appropriate for improved model fitting and biological plausibility and mechanism. A model schematic for TDF and FTC is presented in Figure 1 and Supplemental Figure 1 (Figure S1), respectively. Model progression was based off of a combination of visual inspection of the goodness of fit plots (individual predictions (IPRED) and observation (DV) overlay plots, DV vs IPRED, weighted residuals (WRES) vs population predicted (PRED), WRES vs TIME, CWRES vs PRED, CWRES vs TIME and eta histograms), significant improvement of the objective function value (OFV) (likelihood ratio test, p-value < 0.05), Akaike information criterion (AIC), Bayesian information criterion (BIC), and physiological relevance. A one-compartment and two-compartment blood plasma model was tested for each drug. TDF and FTC included a fixed first order absorption rate constant. Finally, 10/16 TDF SMC and 17/23 FTC SMC samples were pooled per subject due to poor cell recovery, stemming from low semen sample volume.

**TAF—**TAF modeling followed TDF and FTC, with a few key differences. A total of 226 concentration values (n=48 for TAF in BP, n=45 for TFVdp in PBMCs, n=48 for TFV in BP, n=42 for TAF in SP, n=43 for TFV in SP, n=0 for TFVdp for SMCs) were used in the final TAF model. To improve model stability and fitting, relative rate constants (relative to TAF elimination from the BP or SP) were employed to describe TFV disposition. A model schematic for TAF can be found in Figure 1. In addition to TFV and TFVdp concentrations, parent TAF concentrations were measured in the BP and SP. Due to sampling time constraints, the majority of the TAF concentrations were below the limit of quantification (BLQ) following the 6-hour ($2^{nd}$) time point. As such, a likelihood-based approach to handling data below the limit of quantification was applied (24), necessitating the use of the Laplacian estimation with interaction method (25). Finally, all subjects in the TAF arm required pooling of their SMC samples for quantification of TFVdp concentrations. Out of the 8 pooled samples, 5 were BLQ leaving 3 quantifiable samples for modeling of TFVdp in the SMCs. As such, the SMC compartment for the TAF arm was omitted, despite multiple attempts to include it.

**Absorption Rates—**Sample collection restrictions prohibited successful estimation of absorption rates for TDF and FTC models from the data. The time to maximum concentration (Tmax) for TDF and FTC generally occurs prior to the first time point for sample collection at 3 hours. As such, the absorption rate for TFV following TDF administration was set to an arbitrary value of 3.0 $hr^{-1}$ which falls in range with previously reported values (26–29). The absorption rate for FTC was fixed to a previously reported value of 0.6 $hr^{-1}$ (29).

**Volumes of Distribution—**To simplify the model, volumes of distribution for model compartments outside of the BP were assumed to be 1 liter. The central volume of distribution for TAF in the BP was fixed to a previously reported value of 75 L and the total volume of distribution for TFV in the BP following TAF administration was fixed to an estimate of 2000 L based on the approximate estimate of previously reported values for TAF and TFV volume of distributions (15,30).

**Model Validation—**VPCs were constructed with 1,000 simulations using the final parameter estimates from the final base models overlaid with the observed data for each compartment. Bootstrap estimates were obtained from 1,000 replicates generated by repeated random sampling of the original dataset with replacement and were compared to model estimates to evaluate their precision. VPCs and bootstrapping were performed in Perl-Speaks-NONMEM (PsN) version 4.6 or greater (31).

**Data Exclusion—**Observation outliers were determined using the residual plots from the final model. Observations yielding an absolute CWRES value > 6 were considered as outliers and were excluded from the analysis.

## Supplementary Material

Refer to Web version on PubMed Central for supplementary material.

## ACKNOWLEDGEMENTS

The authors would like to thank the study participants, the staff of the UNC Healthcare Infectious Diseases Clinic for assistance with study recruitment, and the staff of the NC TraCS Institute Clinical and Translational Research Center.

We also thank Dr. Angela Kashuba for oversight of drug concentration analysis in the UNC Center for AIDS Research Clinical Pharmacology and Analytical Chemistry Laboratory, and Dr. Brian M. Maas and Ms. Kaitlyn Maffuid for sample processing and laboratory support.

Phoenix Win Nonlin software is generously provided to the Division of Pharmacotherapy and Experimental Therapeutics at the UNC Eshelman School of Pharmacy by Certara, INC, through designation as a Certara Center of Excellence.

Finally, we would like to thank the late Dr. Alan Forrest for his extensive support on the modeling aspects of the study.

FUNDING:

National Institute of Diabetes and Digestive and Kidney Diseases: 5R01DK108424

National Institute of Allergy and Infectious Diseases: 5P30AI050410–20

National Center for Advancing Translational Sciences: UL1TR002489

5R01DK108424 was awarded to MC while JD and HAP and JN were all supported by this award;

5P30AI050410–20 supports CS, APS, and KB; Ronald Swanstrom is the Principal Investigator.

UL1TR002489 supports the NC TraCS Clinical and Translational Research Center, where the research was conducted. The principal investigators are John Buse and Tim Carey.

The content is solely the responsibility of the authors and does not necessarily represent the official views of the NIH.

Dr. Cynthia L. Gay has received research support from Bristol-Myers Squibb, Gilead Sciences, Abbott, Tibotec Therapeutics, Janssen, ViiV Healthcare and Merck

At the time of work, Dr. Stephen Greene and Dr. Jingxian Chen were employees of the UNC Eshelman School of Pharmacy. Currently Dr. Stephen Greene is employed at SK Life Science, Inc. and Dr. Jingxian Chen is employed at Merck.

## REFERENCES

1. Churchill MJ, Deeks SG, Margolis DM, Siliciano RF, Swanstrom R. HIV reservoirs: what, where and how to target them. Nature Reviews Microbiology. 2016;14(1):55–60. [PubMed: 26616417]
2. Hoetelmans RM. Sanctuary Sites in HIV-1 Infection. Antiviral Therapy (London). 1998;3 Suppl 4:13–17.
3. Galvin SR, Cohen MS. Genital Tract Reservoirs. Current Opinion in HIV and AIDS. 2006 3;1(2):162–166. [PubMed: 19372802]
4. Bashiri K, Rezaei N, Nasi M, Cossarizza A. The Role of Latency Reversal Agents in the Cure of HIV: A Review of Current Data. Immunology letters. 2018;196:135–9. [PubMed: 29427743]
5. Stein J, Storcksdieck Genannt Bonsmann M, Streeck H. Barriers to HIV Cure. HLA. Oct 2016;88(4):155–163.
6. Else LJ, Taylor S, Back DJ, Khoo SH. Pharmacokinetics of Antiretroviral Drugs in Anatomical Sanctuary Sites: The Male and Female Genital Tract. Antiviral therapy. 2011;16(8): 1149–1167. [PubMed: 22155899]
7. Imaz A, et al. HIV-1-RNA Decay and Dolutegravir Concentrations in Semen of Patients Starting a First Antiretroviral Regimen. Journal of Infectious Diseases. 2016 11 15;214(10):1512–1519 [PubMed: 27578849]
8. Greener BN, et al. Dolutegravir Pharmacokinetics in the Genital Tract and Colorectum of HIV-Negative Men After Single and Multiple Dosing. Journal of Acquired Immune Deficiency Syndromes. 2013 9 1;64(1):39–44 [PubMed: 23945251]
9. Brown KC, et al. Single- and Multiple-Dose Pharmacokinetics of Darunavir Plus Ritonavir and Etravirine in Semen and Rectal Tissue of HIV-Negative Men. Journal of Acquired Immune Deficiency Syndromes. 2012 10 1;61(2):138–144 [PubMed: 22614898]
10. Klein DM, Evans KK, Hardwick RN, Dantzler WH, Wright SH, Cherrington NJ. Basolateral Uptake of Nucleosides by Sertoli Cells is Mediated Primarily by Equilibrative Nucleoside Transporter 1. The Journal of Pharmacology and Experimental Therapeutics. 7 2013;346(1):121–129. [PubMed: 23639800]
11. Ray AS, Fordyce MW, Hitchcock MJ. Tenofovir Alafenamide: A Novel Prodrug of Tenofovir for the Treatment of Human Immunodeficiency Virus. Antiviral Research. 2016;125:63–70. [PubMed: 26640223]
12. Dumond JB, et al. Differential Extracellular, but Similar Intracellular, Disposition of Two Tenofovir Formulations in the Male Genital Tract. Antiviral Therapy. 2018 10; doi: 10.3851/IMP3277.
13. Lee QA, et al. Selective Intracellular Activation of a Novel Prodrug of the Human Immunodeficiency Virus Reverse Transcriptase Inhibitor Tenofovir Leads to Preferential Distribution and Accumulation in Lymphatic Tissue. Antimicrobial Agents and Chemotherapy. 2005 5;49(5):1898–1906. [PubMed: 15855512]
14. Podany AT, et al. Plasma and Intracellular Pharmacokinetics of Tenofovir in Patients Switched from Tenofovir Disoproxil Fumarate to Tenofovir Alafenamide. AIDS. 2018 3 27;32(6):761–765. [PubMed: 29334548]
15. Luedtke CC, et al. Cathepsin A is expressed in a cell- and region-specific manner in the testis and epididymis and is not regulated by testicular or pituitary factors. J Histochem Cytochem. 2000 8;48(8):1131–46. [PubMed: 10898806]
16. Garrett KL, et al. A Pharmacokinetic/Pharmacodynamic Model to Predict Effective HIV Prophylaxis Dosing Strategies for People Who Inject Drugs. Journal of Pharmacology and Experimental Therapeutics. 2018 11;367(2):245–251. [PubMed: 30150483]

17. Food and Drug Administration. Clinical Pharmacology Review of Genvoya® New Drug Application. Available at: https://www.accessdata.fda.gov/drugsatfda_docs/nda/2015/207561Orig1s000ClinPharmR.pdf. Accessed March 8, 2019.

18. Markowitz M, et al. Phase I/II Study of the Pharmacokinetics, Safety and Antiretroviral Activity of Tenofovir Alafenamide, a New Prodrug of the HIV Reverse Transcriptase Inhibitor Tenofovir, in HIV-Infected Adults. Journal of Antimicrobial Chemotherapy. 2014 5 1;69(5):1362–1369. [PubMed: 24508897]

19. Ruane PJ, et al. Antiviral Activity, Safety, and Pharmacokinetics/Pharmacodynamics of Tenofovir Alafenamide as 10-Day Monotherapy in HIV-1-Positive Adults. Journal of Acquired Immune Deficiency Syndromes. 2013 8 1;63(4):449–455. [PubMed: 23807155]

20. Custodio JM, et al. Pharmacokinetics and Safety of Tenofovir Alafenamide in HIV-Uninfected Subjects with Severe Renal Impairment. Antimicrob Agents Chemother. 2016 8 22;60(9):5135–40. doi: 10.1128/AAC.00005-16. [PubMed: 27216057]

21. Quinney SK, et al. Physiologically based pharmacokinetic model of mechanism-based inhibition of CYP3A by clarithromycin. Drug Metab Dispos. 2010 2;38(2):241–8. doi: 10.1124/dmd.109.028746. Epub 2009 Nov 2. [PubMed: 19884323]

22. Imaz A, et al. Seminal Tenofovir Concentrations, Viral Suppression, and Semen Quality with Tenofovir Alafenamide Compared with Tenofovir Disoproxil Fumarate (Spanish HIV/AIDS Research Network, PreEC/RIS 40). Clinical Infectious Diseases. 2018 12 18 [Epub ahead of print]

23. Simiele M, et al. Evaluation of the Mean Corpuscular Volume of Peripheral Blood Mononuclear Cells of HIV Patients by a Coulter Counter to Determine Intracellular Drug Concentrations. Antimicrobial Agents and Chemotherapy. 2011 6;55(6):2976–2978 [PubMed: 21402849]

24. Beal SL. Ways to Fit a PK Model with Some Data Below the Quantification Limit. Journal of Pharmacokinetics and Pharmacodynamics. 2001;28(5):481–504. [PubMed: 11768292]

25. Bergstrand M, Karlsson MO. Handling Data Below the Limit of Quantification in Mixed Effect Models. The American Association of Pharmaceutical Scientists Journal. 2009;11(2):371–380. doi:10.1208/s12248-009-9112-5. [PubMed: 19452283]

26. Gagnieu MC, et al. Population Pharmacokinetics of Tenofovir in AIDS patients. Journal of Clinical Pharmacology, 2008 48(11): p. 1282–8. [PubMed: 18779377]

27. Lu Y, et al. Population Pharmacokinetics of Tenofovir in HIV-1-Uninfected Members of Serodiscordant Couples and Effect of Dose Reporting Methods. Antimicrobial Agents and Chemotherapy, 2016 60(9): p. 5379–86. [PubMed: 27353269]

28. Burns RN, Hendrix CW, Chaturvedula A. Population Pharmacokinetics of Tenofovir and Tenofovir-Diphosphate in Healthy Women. Journal of Clinical Pharmacology. 2015;55(6):629–638. doi:10.1002/jcph.461. [PubMed: 25581815]

29. Cottrell ML, et al. A Translational Pharmacology Approach to Predicting Outcomes of Preexposure Prophylaxis Against HIV in Men and Women Using Tenofovir Disoproxil Fumarate with or without Emtricitabine. The Journal of Infectious Diseases. 2016 7 1;214(1):55–64. [PubMed: 26917574]

30. Jullien V, et al. Population Pharmacokinetics of Tenofovir in Human Immunodeficiency Virus-Infected Patients Taking Highly Active Antiretroviral Therapy. Antimicrobial Agents and Chemotherapy. 2008 2;53(2):808. [PubMed: 19015333]

31. Lindbom L, Ribbing J, Jonsson EN. Perl-speaks-NONMEM (PsN)--A Perl Module for NONMEM Related Programming. Computer Methods and Programs in Biomedicine. 2004 8;75(2):85–94. [PubMed: 15212851]

## STUDY HIGHLIGHTS

**1.** What is the current knowledge on the topic?

Antiretrovirals penetrate the seminal compartment to varying degrees., determined in part by their physiochemical properties. Nucleoside reverse transcriptase inhibitor (NRTI) concentrations in seminal plasma are generally higher than blood, though knowledge of their active intracellular metabolites in this compartment is limited.

**2.** What question did this study address?

Herein, we gain an understanding of inter- and intra-individual differences in NRTI disposition in blood and semen for tenofovir and its active moiety, tenofovir-diphosphate (TFVdp), following administration of tenofovir alafenamide (TAF) or tenofovir disoproxil fumarate (TDF) through pharmacokinetic modeling.

**3.** What does this study add to our knowledge?

Our findings highlight potentially different patterns of disposition in the male genital tract depending on tenofovir formulation. The complex distributional properties of TAF are reflected in apparent differences in TFV and TFVdp transfer and elimination rates, likely due to a flip-flop kinetics phenomenon. , despite similar intracellular tenofovir diphosphate concentrations in seminal mononuclear cells.

**4.** How might this change clinical pharmacology or translational science?

These findings provide insight into the mechanisms of tenofovir prodrug disposition within the seminal compartment and suggests areas requiring further study as antiretrovirals are considered as part of the “kick and kill” HIV eradication strategy.

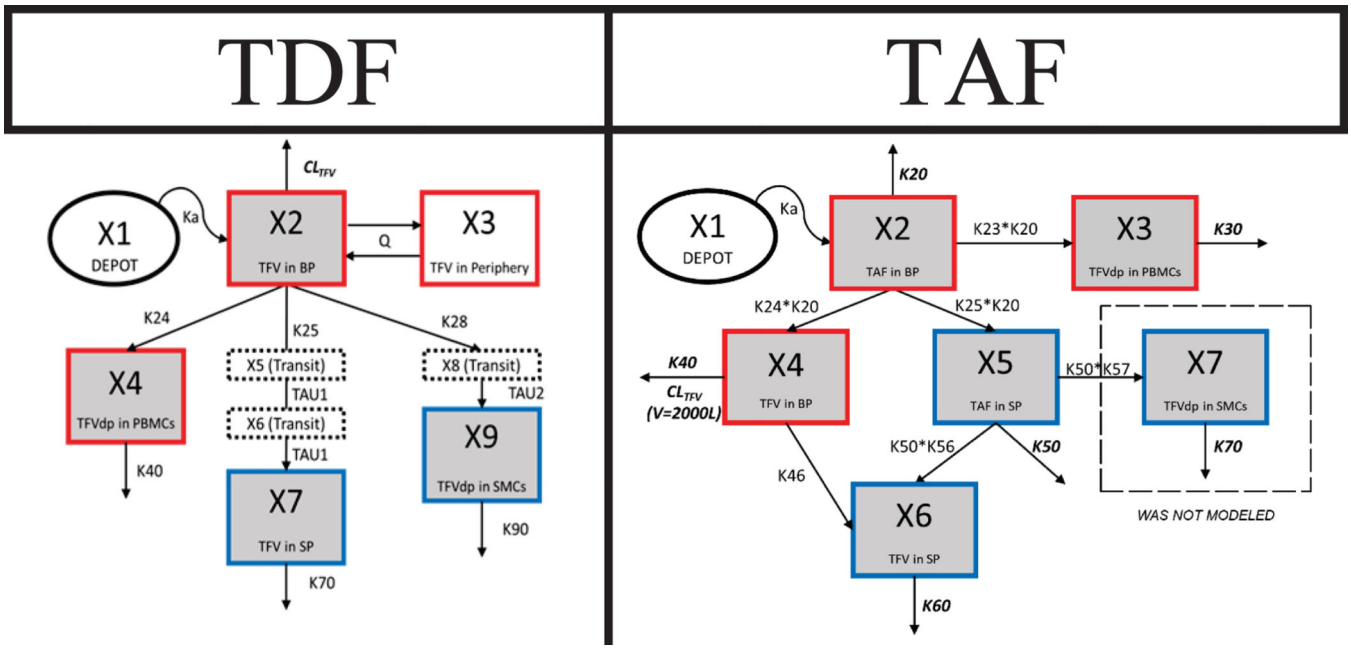


**Figure 1: Model Schematics for Tenofovir Disoproxil Fumarate and Tenofovir Alafenamide**

Red boxes = blood matrices (BP/PBMCs), blue boxes = seminal matrices (SP/SMCs), gray boxes = compartments with direct measurement, doted boxes = transit compartments, dashed box = compartment not modeled, ovals = depot compartments

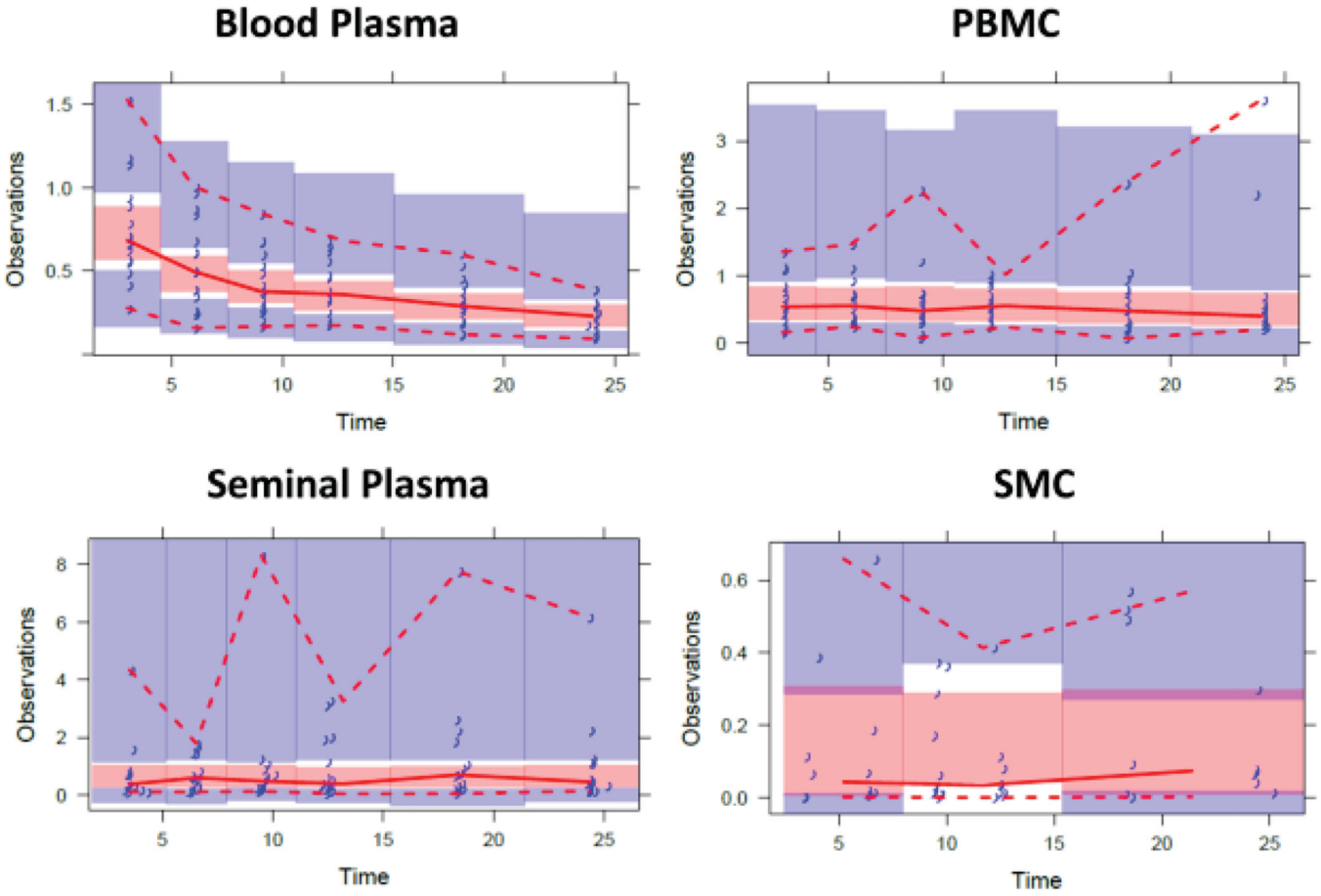


**Figure 2: Visual Predictive Checks for Tenofovir Disoproxil Fumarate**

Blue markers = observed data, red dashed lines = predicted 5$^{th}$ and 95$^{th}$ prediction lines, red solid line = median prediction line, red and blue shaded regions = 95% confidence intervals

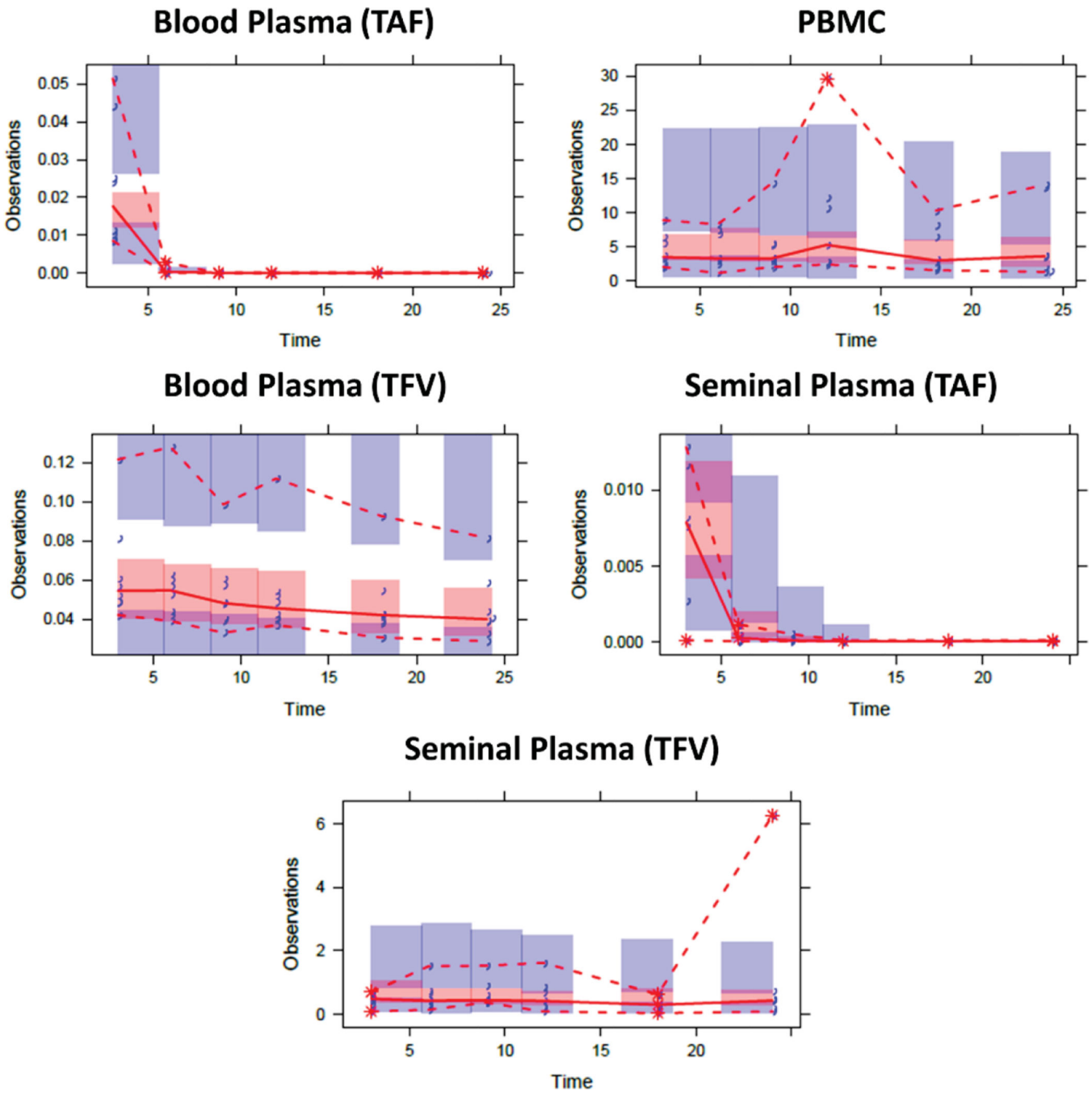


**Figure 3: Visual Predictive Checks for Tenofovir Alafenamide**

Blue markers = observed data, red dashed lines = predicted 5$^{th}$ and 95$^{th}$ prediction lines, red solid line = median prediction line, red and blue shaded regions = 95% confidence intervals

**Table 1:**

Population Pharmacokinetic Estimates for Tenofovir Disoproxil Fumarate (TDF)

| Parameter (units) | Final NONMEM Estimate | Median Bootstrap Estimate | Bootstrap 95% CI | %RSE |
|---|---|---|---|---|
| Ka ($hr^{-1}$) * | 3 | 3 | -- | -- |
| CL/F (L/hr) | 40.4 | 39.7 | (26.1 – 50.3) | 17.7% |
| V/F (L) | 161 | 154 | (26.7 – 291) | 47.6% |
| Q/F (L/hr) | 73.6 | 64.0 | (20.8 – 119) | 44.8% |
| V2/F (L) | 618 | 574 | (275 – 839) | 29.4% |
| K24 ($hr^{-1}$) | 0.0344 | 0.0394 | (0.00567 – 0.106) | 75.0% |
| K40 ($hr^{-1}$) | 0.0309 | 0.0364 | (0.00577 – 0.0910) | 72.7% |
| K25 ($hr^{-1}$) | 0.0152 | 0.0114 | (0.00234 – 0.0153) | 80.8% |
| TAU1 ($hr^{-1}$) | 0.001 | 0.00100 | (0.000994 – 0.00103) | 1030% |
| K70 ($hr^{-1}$) | 0.0126 | 0.00992 | (0.00208 – 0.0127) | 99.9% |
| K26 ($hr^{-1}$) | 0.0263 | 0.0248 | (0.00608 – 0.0507) | 59.5% |
| TAU2 ($hr^{-1}$) | 0.0845 | 0.0864 | (0.0409 – 0.455) | 138% |
| K80 ($hr^{-1}$) | 0.0844 | 0.0812 | (0.0236 – 0.159) | 63.4% |
| ω on CL/F (%CV) | 26.3% | 24.0% | (8.98% – 35.7%) | 49.8% |
| ω on V/F (%CV) | 82.8% | 84.7% | (15.5% – 166%) | 95.2% |
| ω on K40 (%CV) | 42.0% | 37.8% | (8.36% – 65.0%) | 64.6% |
| ω on K50 (%CV) | 88.9% | 83.5% | (50.1% – 110%) | 35.0% |
| o on BP (%CV) | 21.4% | 21.1% | (13.8% – 29.5%) | 42.2% |
| o on PBMC (%CV) | 52.2% | 51.5% | (39.5% – 66.3%) | 24.8% |
| o on SP (%CV) | 43.9% | 44.1% | (38.0% – 49.5%) | 12.7% |
| o on SMC (%CV) | 145% | 137% | (99.4% – 168%) | 24.9% |

* Fixed Parameter

95% CI – 95% Confidence Interval of bootstrap estimate

%RSE – Relative Standard Error in Percentage Terms

ω – Interindividual Variability

o – Residual Variability

%CV – Coefficient of Variation in Percentage Terms

**Table 2:**

Population Pharmacokinetic Estimates for Tenofovir Alafenamide (TAF)

| Parameter (units) | Final NONMEM Estimate | Median Bootstrap Estimate | Bootstrap 95% CI | %RSE |
|---|---|---|---|---|
| Ka ($hr^{-1}$) | 2.08 | 2.03 | (1.57 – 2.46) | 23.6% |
| $V_{TAF}$ (L)* | 75.0 | 75.0 | -- | -- |
| K20 ($hr^{-1}$) | 1.20 | 1.23 | (1.16 – 1.45) | 5.43% |
| K23 ($hr^{-1}$) | 0.0489 | 0.0479 | (0.0000153 – 0.090) | 28.8% |
| VTFV (L)* | 2000 | 2000 | -- | -- |
| K30 ($hr^{-1}$) | 0.0130 | 0.0124 | (0.00000395 – 0.0337) | 36.0% |
| K24 ($hr^{-1}$) | 1.07 | 1.08 | (0.795 – 1.72) | 12.9% |
| K40 ($hr^{-1}$) | 0.00215 | 0.00230 | (0.000101 – 0.0109) | 55.0% |
| K25 ($hr^{-1}$) | 0.000943 | 0.000963 | (0.000692 – 0.00213) | 68.2% |
| K50 ($hr^{-1}$) | 0.762 | 0.625 | (0.602 – 1.13) | 21.8% |
| K46 ($hr^{-1}$) | 0.00952 | 0.00947 | (0.00145 – 0.0135) | 17.0% |
| K56 ($hr^{-1}$) | 0.000256 | 0.000523 | (0.0000102 – 0.00716) | 643% |
| K60 ($hr^{-1}$) | 1.97 | 1.98 | (0.244 – 3.21) | 20.2% |
| ω on K30 (%CV) | 74.5% | 67.9% | (20.9% - 94.3%) | 29.4% |
| ω on K40 (%CV) | 120% | 113% | (16.7% - 185%) | 55.9% |
| ω on K50 (%CV) | 38.3% | 48.91% | (0.0976% - 48.92%) | 23.3% |
| ω on K60 (%CV) | 85.4% | 84.5% | (3.15% - 118%) | 40.4% |
| o on TAF BP (%CV) | 86.1% | 95.6% | (55.7% - 150%) | 184% |
| o on PBMC (%CV) | 56.0% | 52.6% | (32.5% - 79.3%) | 28.3% |
| o on TVF BP (%CV) | 10.9% | 10.9% | (8.16% - 12.1%) | 9.87% |
| o on TAFSP(%CV) | 51.7% | 55.4% | (32.8% - 66.2%) | 995% |
| o on TVF SP(%CV) | 48.6% | 44.6% | (26.9% - 69.8%) | 30.4% |
| o on SMC (%CV) | Not Applicable | | | |

*Fixed Parameter

95% CI - 95% Confidence Interval of bootstrap estimate

%RSE – Relative Standard Error in Percentage Terms

ω – Interindividual Variability

o – Residual Variability

%CV - Coefficient of Variation in Percentage Terms

**Table 3:**

Comparison of Model Estimates Between TDF and TAF

| Parameter (TDF vs TAF) | TDF | TAF | TAF Fraction (%) |
|---|---|---|---|
| TFV CL/F from BP (L/hr) | 40.4 | 4.60 * | 11.3% |
| TFVdp elimination from PBMCs ($hr^{-1}$) (K40 vs K30) | 0.0309 | 0.0124 | 40.1% |
| Transit of TFV from BP to SP ($hr^{-1}$) (K25 vs K46) | 0.0152 | 0.00947 | 62.3% |
| Elimination of TFV from the SP ($hr^{-1}$) (K50 vs K60) | 0.0126 | 1.98 | 15,700% |

*=based on a fixed TFV volume of distribution of 2000 L